

Electron-phonon interaction in individual strain-free GaAs/Al_{0.3}Ga_{0.7}As quantum dots

S. Sanguinetti, E. Poliani, M. Bonfanti, M. Guzzi, and E. Grilli

Dipartimento di Scienza dei Materiali and CNISM, Università di Milano Bicocca, Via Cozzi 53, I-20125 Milano, Italy

M. Gurioli

L.E.N.S., Dipartimento di Fisica and CNISM, Università di Firenze, Via Sansone 1, I-50019 Sesto Fiorentino, Italy

N. Koguchi

National Institute for Materials Science, 1-2-1 Sengen, Tsukuba, Ibaraki 305-0047, Japan

(Received 24 May 2005; revised manuscript received 21 November 2005; published 27 March 2006)

We report accurate measurements of the excitonic ground state transitions in individual, strain free, GaAs/Al_{0.3}Ga_{0.7}As quantum dots. We determine the spectral width and the energy of the zero-phonon line as a function of the temperature for a series of quantum dots with different sizes. In particular, the thermal broadening is well reproduced by a thermally activated process having a single activation energy (36 meV, corresponding to the GaAs LO phonon energy) independently of the dot size. Similarly, the energy of the zero-phonon line follows the GaAs gap temperature dependence irrespective of the dot size. Our findings demonstrate that (a) the exciton decoherence in quantum dots cannot be attributed to inelastic electron-phonon scattering but rather to pure dephasing processes driven by GaAs-LO phonons and (b) there is no quantum size effect on the excitonic energy renormalization with the temperature.

DOI: [10.1103/PhysRevB.73.125342](https://doi.org/10.1103/PhysRevB.73.125342)

PACS number(s): 78.67.Hc, 78.55.Cr, 73.21.La, 71.38.-k

I. INTRODUCTION

Recent observations of Rabi oscillations¹⁻³ and photon antibunching^{4,5} in single semiconductor quantum dots (QDs) have demonstrated the remarkable similarity of QDs to atomic systems. This makes the QDs potentially basic elements both for novel optoelectronic nanodevices and for quantum information technologies. However, carriers in semiconductor QDs, contrary to isolated atoms, couple to the vibrational modes of the crystal lattice. Charges localized in the QD efficiently interact with lattice vibrations via acoustic and optical phonons⁶⁻¹² and polaronic effects indeed play a major role in many aspects of the QD carrier dynamics and recombination kinetics.¹³⁻¹⁶ On one side, this produces relevant advantages: the strong lattice interaction is at the origin of the lack of phonon-bottleneck effect in QDs,¹³ thus making the QD laser highly efficient. On the other side, electron-phonon interaction plays a dominant role in the QD electronic states decoherence¹⁷⁻²¹ which is the main limitation in quantum information processing. It follows that a good knowledge of the electron-phonon interaction (EPI) in QDs is of the utmost importance.

Despite intense research efforts for achieving a deeper understanding of the EPI mechanism in strongly confined systems, such as III-V QDs, there are still important open questions. By means of the single QD emission lineshape and energy measurements as a function of the temperature it is possible to access information about two relevant EPI driven effects: excitonic homogeneous broadening and energy renormalization.

As far as the excitonic homogeneous broadening in QDs is concerned, it is well known that the single QD emission spectrum consists of a sharp line, which dominates at low T , and of a broader pedestal (spectral sidebands), whose relative intensity is growing with T .^{6,10,11} The most accepted picture

of the T dependence of the homogeneous linewidth is based on the so-called independent boson model^{10,22,23} (IBM). The IBM attributes the narrow band at low T as the zero-phonon line (ZPL) while the non-Lorentzian sidebands appearing at high T are interpreted in the framework of a polaronic picture. Although IBM does not predict any dependence on T of the ZPL linewidth, experiments report a noticeable ZPL linewidth increase with the temperature.^{6,24,25} Most of the experimental works report temperature-activated behaviors of the ZPL linewidth, with activation energies spread in the 15–36 meV range.^{6,9,10,24,26} Different values have been attributed either to scattering with different kinds of LO phonons (bulk, localized, or alloy phonons), or to the promotion of excitons into excited states. An important point to make is that the majority of the studies of QD excitonic dephasing have been performed in InGaAs/GaAs Stranski-Krastanow (SK) QDs, where the possible relevance of the strain may obscure the intrinsic EPI in QDs. Generally speaking, when considering the excitonic dephasing, two different mechanisms can be distinguished: (1) inelastic dephasing processes, such as phonon-assisted transfer of carriers to excited electronic states or interband recombination and (2) elastic interaction with phonons (pure dephasing processes), which does not change the carrier occupation, associated with the nondiagonal terms in the interaction with acoustic²⁰ or optical^{18,21} phonons. Contrary to pure dephasing mechanisms, inelastic dephasing is expected to depend on the QD energy level spacing. Then quantum size effects on the T dependence of the dephasing time could be used to discriminate between the two dephasing mechanisms. Borri *et al.*²⁵ have already addressed this problem via four wave mixing (FWM) measurements of the polarization decay in QDs showing that the dephasing time does not depend, at high T , on the confinement energy. They concluded that the elastic scattering likely plays a major role for exciton dephasing,

even if the observed activation energy of the dephasing process does not correspond to any of the modes in the vibrational spectrum of the InGaAs system.²⁵

Much less attention has been paid to the band gap renormalization in QDs. Excitons localized in quantum well fluctuations have been used to perform high-precision determination of the T -dependent band-gap shrinkage²⁷ due to their sharp emission lines. However, no strong EPI modification is, *a priori*, expected in these systems, due to the weak localization regime of the localized excitons.²⁸ On the other side, the effect of quantum confinement on the T renormalization of the excitonic transition energy of III-V QDs in the regime of strong confinement is not yet understood in deep detail. *A priori*, the QD temperature dependence of the fundamental optical transition is expected to be different from that of bulk semiconductors.²⁸ From the theoretical point of view, the renormalization of excitonic energies by EPI (Ref. 29) should be stiffened by the quantum confinement,²⁸ thus inducing a quantum size effect on the T dependence of the QD excitonic emission. As a matter of fact, size variation deeply changes the electronic structure and the electronic wave function, which are fundamental quantities in determining the strength and the behavior of the EPI. However, no experimental evidence of major changes of the T dependence of the energy gap in the lattice-matched III-V QDs has been insofar reported.^{30–32}

In this work we present a detailed and systematic investigation of the temperature dependence of homogeneous broadening and energy transition of single QD emission as a function of the QD size. The investigated sample is a GaAs/Al_{0.3}Ga_{0.7}As QD structure grown by modified droplet epitaxy (MDE).^{33–35} The use of GaAs/Al_{0.3}Ga_{0.7}As MDE-QDs has three main advantages with respect to the InGaAs/GaAs SK QDs: (1) the exact composition of the QD is known, on the contrary, to In(Ga)As/GaAs SK-QDs, where segregation effects play a major role in determining the In content of the QD.³⁶ (2) The GaAs/Al_{0.3}Ga_{0.7}As QDs can be considered almost strain-free in all the investigated temperature range due to the negligible lattice and thermal expansion mismatch between the Al_{0.3}Ga_{0.7}As barrier and the GaAs QD.³⁷ In InGaAs/GaAs SK QDs size-dependent strain effects cannot be neglected, thus inducing additional uncontrolled parameters to the systems. (3) The MDE possibility to tune and control the QD density was used to grow samples at low QD density but with large size dispersion allowing the selection of individual QDs with strongly different sizes within a single sample, by means of microphotoluminescence (μ -PL) measurements.

We show that the exciton dephasing in strain-free single QDs is independent of the confinement energy, and follows a thermally activated behavior with an activation energy of ≈ 36 meV, which corresponds to the GaAs bulk LO optical phonon. This finding, which supports the interpretation of exciton decoherence as due to pure dephasing,^{18,20,21} shows the important role played by bulk LO phonons in determining the exciton decoherence. In addition, we were able to follow with high precision the QD band gap shrinking with increasing temperature up to 115 K in QD with strongly different sizes. No change from the GaAs bulk temperature dependence has been observed. This observation implies a

small, if any, quantum confinement effect on the renormalization of band energies by EPI for excitons in the strong localization regime, on the contrary of what has been found in lead salt QDs.²⁸

II. SAMPLES AND EXPERIMENT

The investigated GaAs/Al_{0.3}Ga_{0.7}As QD sample (named B580) was grown by MDE in a conventional molecular beam epitaxy apparatus. MDE is a growth method for self-assembling QDs even in lattice matched systems.³⁴ After the growth of 500 nm Al_{0.3}Ga_{0.7}As barrier layer at 580 °C by molecular beam epitaxy, the substrate temperature was lowered to 350 °C, the As valve closed and the As pressure in the growth chamber depleted. At this temperature and in absence of As, the initially deposited Ga atoms are incorporated into the arsenic terminated $c(4 \times 4)$ surface³⁸ resulting in the appearance of a Ga stabilized surface. Subsequent Ga deposition gives rise to the formation of tiny Ga droplets on the substrate. The total amount of deposited Ga was equivalent to the Ga quantity necessary to obtain 1.2 ML of GaAs in the presence of As. Following the deposition of the droplets the temperature was lowered to 180 °C and an As₄ molecular beam with the flux of 2×10^{-4} Torr was irradiated on the surface. This growth step causes the complete arsenization of the Ga droplets and thus the formation of pyramidal shaped nanocrystals on the surface. After the complete change of reflection high-energy electron diffraction (RHEED) pattern from halo to spots, which corresponds to the complete arsenization of the Ga droplet, an Al_{0.3}Ga_{0.7}As barrier layer of 10 nm was grown by migration enhanced epitaxy³⁹ at the same temperature of 180 °C. This temperature was chosen in order to prevent two-dimensional regrowth of the naked GaAs nanocrystals.³⁴ Then, the growth temperature was raised back to 580 °C and 90 nm of Al_{0.3}Ga_{0.7}As and 10 nm of GaAs as cap layer were grown by ordinary molecular beam epitaxy. The sample was then annealed in 1.5×10^{-5} Torr As₄ atmosphere at 580 °C for 1 h.

A QD density of the order of $\approx 6 \times 10^8$ cm⁻² was measured by surface high resolution scanning electron microscope (HRSEM) on uncapped samples. Cross-sectional HRSEM images, after annealing, demonstrate the formation of pyramidal shape nanocrystals of ≈ 16 nm height and ≈ 20 nm base.³⁵ Magneto-photoluminescence measurements performed on a similar sample confirm the excitonic localization with an exciton Bohr radius of 7.3 nm. The detailed description of the sample growth and its optical characterization can be found in Ref. 35.

We performed temperature-dependent photoluminescence (PL) measurements for several single QDs under nonresonant excitation in the AlGaAs barrier. The sample was placed in a cold-finger helium flow cryostat which allows to vary the temperature between 5 K and room temperature. μ -PL measurements were performed in the far field using a microscope objective (numerical aperture 0.4). The nonresonant excitation beam [Nd:YAG (yttrium aluminum garnet) duplicated laser $-\lambda_{\text{exc}} = 532$ nm] was focused on the sample with a spot size of 1 μ m, accurately positioned using X-Y-Z translation stages moving the cryostat with a precision 0.1 μ m.

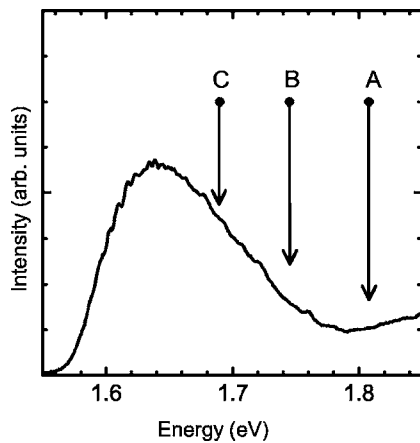


FIG. 1. Broad area PL emission of the sample B580. The arrows indicate the energy position of the measured single QDs.

The excitation power density was in the range 1–100 W/cm². The emission, collected by the same objective, was dispersed by a double grating spectrometer. The signal is detected by a Peltier-cooled Si charged-coupled device camera. The spectral resolution was 90 μ eV.

It is worth noticing that, around ten QDs are expected inside the detection area and then no sample preparation with mesa was needed in order to separate the contributions coming from different QDs, thus ruling out extrinsic effects connected with the mesa preparation.⁴⁰

Figure 1 shows the broad area PL emission (laser spot diameter of the order of 1 mm) at $T=10$ K from MDE-QDs, which consists of a large band, centered at 1.64 eV with a full width at half maximum (FWHM) of 130 meV due to the strong inhomogeneous broadening inherent to the growth process. The spread of QD size allows us to measure very different QDs within the same samples. In order to select exciton recombination in strong confinement condition, we have concentrated our analysis on the high energy side of the PL band from the QD ensemble. In particular, we selected three QDs, denoted as follows: QDA (1.808 eV), QDB (1.745 eV), and QDC (1.69 eV), whose energies are defined by arrows in Fig. 1. The chosen QDs have emission lines spectrally well separated by the PL lines arising from spatially neighboring QDs.

Figure 2(a) shows the μ -PL spectra of QDA at $T=10$ K. The emission of the individual QD consists of a single sharp peak, whose line shape is better reproduced by a Gaussian profile with respect to a Lorentzian profile (see the inset of Fig. 2). Increasing the excitation power density the QD PL emission turns into a multiplet [see the inset of Fig. 2(b)], which stems from the multiexcitonic nature of the emission at high injection levels. The summary of the FWHM γ obtained from the investigated QDs at low T is shown in Fig. 3. Despite the large spread of the data, denoting a major role of environment disorder on γ , we remark on an increase of the linewidth as the emission energy decreases; larger QDs tend to show larger linewidth.

The measured PL spectra at different temperatures of the three selected QDs are reported in Fig. 4. The low temperature linewidths are 130 μ eV, 280 μ eV, and 300 μ eV for

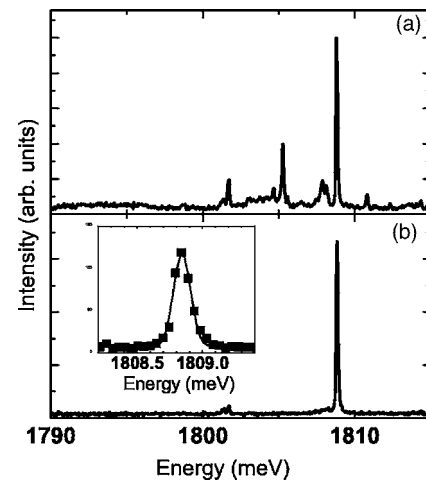


FIG. 2. (a) and (b) QDA PL spectrum at $T=10$ K and excitation power density $P_{\text{exc}}=1$ W/cm² (a) and $P_{\text{exc}}=100$ W/cm² (b), respectively. Inset: QDA PL spectrum at $T=10$ K and $P_{\text{exc}}=1$ W/cm² with its Gaussian fit.

QDA, QDB, and QDC, respectively. As already stated, within the IBM framework, the narrow line clearly visible in the low T is attributed to the ZPL emission from the QDs. As the temperature increases, the ZPL emission redshifts and quenches. We compensated the thermal reduction of the average QD carrier population by increasing the excitation power density, thus working at nearly constant emission intensity. We carefully checked that the increase of the excitation power density did not affect the PL line shape introducing multiexcitonic effects. For all the QDs the PL band remains characterized, up to 65 K, by a single line, whose width slowly increases with the temperature. Around 65 K the non-Lorentzian sidebands start to appear and their relative intensity increases with the temperature. We also note that, at constant temperature, the importance of the sidebands decreases with decreasing QD emission energy and that a slight asymmetry between the low and high energy sideband, with a predominance of the low energy tail, is observed. Finally, above 100 K, the QD emission is dominated by the sideband contribution.

The ZPL linewidth and peak energy of the three QDs in the whole measured T range, obtained by line shape fits, are reported in Figs. 5 and 6, respectively.

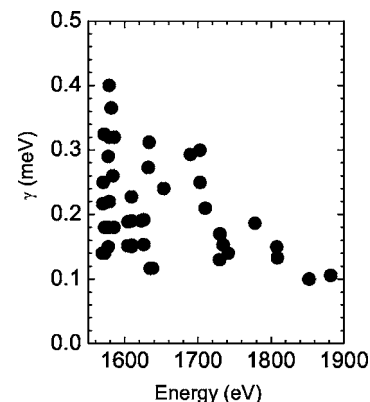


FIG. 3. Excitonic emission linewidth at $T=10$ K as a function of the PL emission energy.

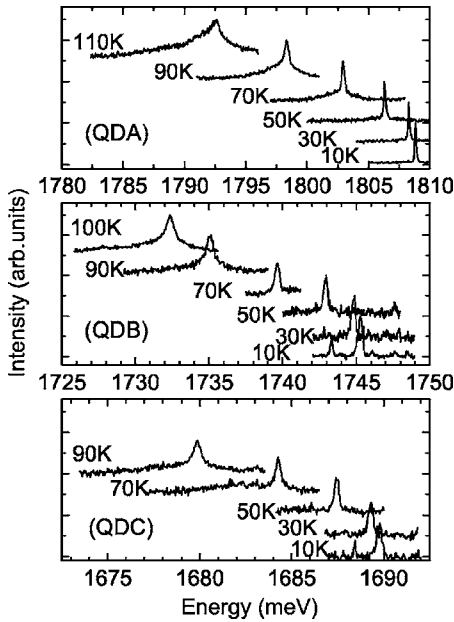


FIG. 4. PL emission of the single quantum dots at different temperatures: QDA (upper panel), QDB (central panel), and QDC (bottom panel). The measurement temperatures are indicated by labels. Each spectrum is normalized to its maximum.

III. DISCUSSION

According to Ref. 35 it is possible to relate, by means of a simple model based on the effective mass approximation, the emission energy with the QD size. In particular, assuming a constant QD height to base ratio of 0.8,³⁵ QDA emission corresponds to a QD with a base size of ≈ 14 nm, QDB ≈ 20 nm, and QDC ≈ 24 nm, respectively. This places our QDs well inside the range of sizes dominated by strong electronic confinement, and, at the same time, the three chosen QDs allow us to span a quite large QD size range. Let us also remark that the annealing procedure, used to improve the MDE-QD emission yield, produces a sizable interdiffusion

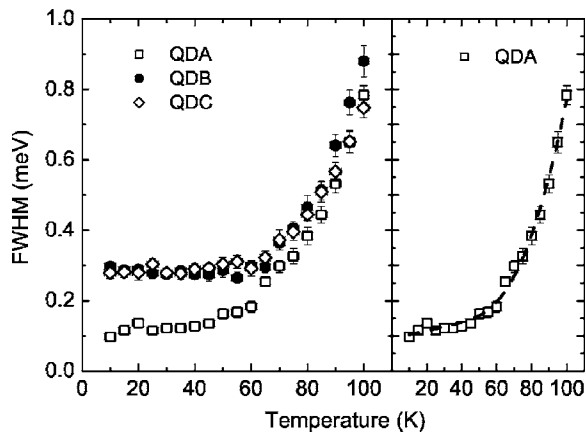


FIG. 5. Left panel: temperature dependence of the ZPL excitonic emission linewidth of QDA (squares), QDB (circles), and QDC (diamonds). Right panel: temperature dependence of the ZPL excitonic emission of QDA together with the fit (dashed line) obtained using Eq. (1) with the parameters reported in Table I.

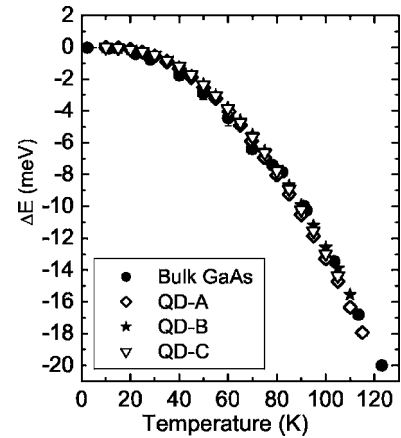


FIG. 6. Temperature dependence of the ZPL excitonic emission energy of QDA (diamonds), QDB (stars), and QDC (triangles). The bulk GaAs gap (circles) (Ref. 48) is also reported for comparison.

(≈ 1 nm) only at the QD-barrier interface.³⁵ In most of the QDs in the ensemble, interdiffusion just affects the QD surface with the sole effect of changing the QD effective size. Interdiffusion affecting the QD core, thus changing the QD composition, are expected for QDs whose size is well below 10 nm, thus with an emission energy above ≈ 1.85 eV.³⁵

The analysis of the T dependence of the individual QD emission in terms of linewidth and energy gives us access to two different aspects of the EPI in strongly confined systems. Therefore, we split the discussion in two separate sections: excitonic homogeneous linewidth and excitonic energy.

A. Excitonic linewidth

The low temperature linewidth γ of the excitonic ZPL is, for all the three QDs, larger than both the instrumental resolution ($90 \mu\text{eV}$) and the expected intrinsic linewidth (few μeV). We attribute this to local QD environment effects,²⁴ such as spectral diffusion.^{41,42} This also explains the spread of γ shown in Fig. 3, as already reported in Ref. 43 and attributed to the environment disorder. The observed increase of the low- T ZPL linewidth with the QD size can be interpreted within the same framework, since a more relevant influence of the environment may be expected for larger QDs.³⁵ The observed Gaussian line shape of the ZPL in all the three QDs is, again, in agreement with the interpretation of the inhomogeneous broadening due to spectral diffusion.

The Gaussian line shape is maintained up to ≈ 50 K. The linewidths, in the 10–50 K range, show just a slight dependence on T . As the temperature increases, the QD emission shows two sidebands whose intensity is increasing with T . We identify the broad sidebands appearing at high T in the framework of the IBM predictions.^{10,22,23} According to IBM theory, the smaller is the QD, the larger the coupling with the acoustic phonons.¹⁹ This prediction is clearly fulfilled by our observation, where the spectral weight of the acoustic sidebands decreases for increasing QD dimensions.

Strikingly, the ZPL shows similar T behaviors in all the three QDs. Above ≈ 70 K the ZPL width increases showing a temperature activated broadening, with the three QDs show-

TABLE I. Fit parameter set for Eq. (1).

	γ_0 (μeV)	a ($\mu\text{eV}/\text{K}$)	b (meV)	E_A (meV)
QDA	92 ± 13	1.1 ± 0.4	35 ± 12	35 ± 3
QDB	300 ± 10	-0.6 ± 0.3	58 ± 15	38 ± 3
QDA	280 ± 10	0.2 ± 0.2	37 ± 10	37 ± 3

ing, at high T , roughly the same spectral linewidth.

We fit the observed ZPL broadening with the phenomenological temperature activated formula^{6,44}

$$\gamma(T) = \gamma_0 + aT + b[\exp(E_A/k_B T) - 1], \quad (1)$$

where E_A is the activation energy for the scattering process. In the literature, the presence of the linear term in Eq. (1) has been widely reported,^{8,9,24,40,46} even if the parameter a depends on the local QD environment.^{24,40} In the quantum well case, the linear temperature term accounts for exciton absorption of acoustic phonons of energies much smaller than $k_B T$.⁴⁵ In the QD case, because of the lack of excited states, this term should assume a different meaning and its origin is still matter of debate.

The typical fitting curve at the experimental data, by using Eq. (1), is reported (dashed line) in Fig. 5. The fit parameters for all the three QDs are listed in Table I. We note that the activation energy E_A is, within the experimental error, compatible with the optical LO phonon energy (36 meV) in GaAs. It must be pointed out that no strain-related deformations of the phonon spectrum are expected in our QDs due to their strain-free nature. Also the b coefficient is fairly the same, at least within the uncertainties, in the three QDs. On the contrary, the value of a is almost undetermined due to the large inhomogeneous broadening that hides the thermal broadening at low T .

The T dependence of the ZPL linewidth, as a function of QD size, has been reported recently via FWM dephasing experiments in ensembles of SK-QDs,²⁵ where the QD size was modified by means of rapid thermal annealing; the measurements were then performed on different samples. On the contrary, in our experiments we have directly measured the ZPL linewidth T behavior of individual QDs within the same sample. Nethertheless the same overall picture emerges: (a) the independence of the ZPL excitonic dephasing time from the QD size, and, in turn, from its electronic structure; (b) the ZPL linewidth shows, above 60 K, a temperature-activated behavior with an activation energy close to that of the GaAs-LO phonons ($E_A=28$ meV in Ref. 25 and $E_A=36$ meV in this work).

The very similar temperature dependence of the ZPL in different QDs poses some constraints on the interpretation of the effect. The excitonic promotion from the ground state into higher energy states via one-phonon absorption would require electronic states at the LO phonon energy and this is not the case. For instance, QDA, the smaller of the QDs, has already quite a large confinement energy (160 meV) which pushes the first excited electronic state well above the LO phonon energy. Pure dephasing by elastic phonon scattering, which does not depend on the exact electronic structure of

the QDs, can be regarded as the likely processes for exciton decoherence and, at the same time, the GaAs-LO phonon plays the leading role. According to Refs. 18 and 21, elastic scattering by LO phonon with a finite lifetime, owing to the decay into acoustic phonons, predicts a temperature behavior of the ZPL linewidth at low T in qualitative agreement with our findings. However, the predicted b prefactor^{18,21} is more than one order of magnitude lower than the one estimated from our data.

B. Excitonic energy

EPI determines also the thermal shrinking of the fundamental optical transition of QDs $E_{ZPL}(T)$. As shown by Olkhovets *et al.*,²⁸ the size-dependent temperature variation of excitonic emission has been observed in lead-salt QDs. A sizable contribution to the observed size dependence was re-conducted to EPI related effects.

As a matter of fact, in bulk semiconductors the mechanisms that are responsible for the temperature dependence of the electronic bands at constant pressure are the renormalization of band energies by EPI and the thermal expansion.²⁹ Self-energy terms,⁴⁷ which are connected to electron-phonon scattering events, are expected to be modified, with respect to the bulk case, by the atomlike electronic density of states of the QDs.²⁸ In addition, the wave-function localization in the strong confinement regime should also influence, together with the electronic structure, the spectrum of interacting phonons (see, e.g., Ref. 19).

Generally speaking, further QD specific effects may play a role in determining the $E_{ZPL}(T)$,²⁸ such as the temperature-dependent strain due to the mismatch of the thermal lattice expansion between the QD and the host material. However, GaAs/Al_{0.3}Ga_{0.7}As QDs are lattice-matched heterostructures and the mismatch of the thermal expansion coefficients between the QD and the barrier material is below 3%. So we can disregard these specific QD mechanisms as possible sources of change of QD- $E_{ZPL}(T)$ with respect to the bulk case.

Thus possible quantum size effects, completely ascribable to EPI modifications by quantum confinement, may be observable in the $E_{ZPL}(T)$ of GaAs/Al_{0.3}Ga_{0.7}As QDs and following Ref. 28, the effect is expected to be quite strong; however, this is not the case.

The ZPL energy T dependence of the measured QDs is reported in Fig. 6. Strikingly, the data of the three QDs agree within the experimental errors. For the sake of comparison, in the same figure are also reported the original data of a high precision experimental study on the thermal shrinkage of the bulk GaAs gap;⁴⁸ the agreement with QD data is also excellent. We must conclude that no quantum size effect is observed. It is possible to speculate that the differences between PbS-QDs (Ref. 28) and GaAs-QDs reported here may be related to the smaller exciton Bohr radius of GaAs ($a_B^{\text{GaAs}} \approx 10$ nm) with respect to PbS ($a_B^{\text{PbS}} \approx 46$ nm). However a sound theoretical support would be needed for a quantitative interpretation of our results. Very recently the T dependence of the excitonic emission in In(Ga)As/GaAs SK-QDs has been reported.³² Small deviations of $E_{ZPL}(T)$ from

the band gap shrinkage of the nominal In(Ga)As bulk material have been observed and attributed to the different coupling of QDs with long wavelength phonons.³² In our samples, despite the accuracy of both the QDs and GaAs bulk data, we cannot observe such deviations. We guess that the discrepancies found in Ref. 32 have to be attributed to strain-related phenomena. The mismatch of the lattice thermal expansion between InAs and GaAs is about $\approx 21\%$. In addition, as already pointed out, in SK-QDs the exact composition, as well as the residual strain, is not known with high accuracy³⁶ thus making questionable the comparison with the bulk material.

IV. CONCLUSIONS

In conclusion, we have presented a detailed and systematic analysis of the T dependence of the single QD emission as a function of the QD size in strain-free, GaAs/AlGaAs QDs. In particular, we have analyzed the ZPL temperature behavior in terms of linewidth and peak energy. These quantities are of particular relevance being both connected with the nature of EPI.

At low temperatures the ZPL width stems from spectral diffusion, whose relevance increases with the QD size, ac-

ording to the higher defectivity of the larger QDs. As the temperature increases the single QD emission undergoes significant modifications also connected to the appearance of acoustic sidebands, whose intensity decreases as the QD size increases, in agreement with IBM theories.¹⁹ The ZPL shows a remarkable increase, when increasing the temperature, of the linewidth connected to thermally activated dephasing processes. The activation energy nicely corresponds to the GaAs-LO phonon energy (36 meV) independently of different size. These findings support the interpretation of exciton decoherence as due to pure dephasing with the activation of elastic scattering of carriers into virtual states by phonons.^{18,20,21}

The dependence of the ZPL energy on T has been determined with high precision in the 10–110 K range. The ZPL follows, within the experimental errors, the GaAs bulk gap dependence on the temperature, irrespective of the QD size. This shows that the EPI mechanisms which determine the excitonic energy renormalization with the temperature is not strongly affected by electron confinement in our QD size range. We think that our findings should stimulate further theoretical works on the role of quantum confinement on the excitonic energy renormalization by EPI.

-
- ¹T. H. Stievater, X. Li, D. G. Steel, D. Gammon, D. S. Katzer, D. Park, C. Piermarocchi, and L. J. Sham, *Phys. Rev. Lett.* **87**, 133603 (2001).
- ²H. Kamada, H. Gotoh, J. Temmyo, T. Takagahara, and H. Ando, *Phys. Rev. Lett.* **87**, 246401 (2001).
- ³H. Htoon, T. Takagahara, D. Kulik, O. Baklenov, A. L. Holmes, and C. K. Shih, *Phys. Rev. Lett.* **88**, 087401 (2002).
- ⁴P. Michler, A. Kiraz, C. Becher, W. V. Schoenfeld, P. M. Petroff, L. Zhang, E. Hu, and A. Imamoglu, *Science* **290**, 2282 (2000).
- ⁵C. Santori, M. Pelton, G. Solomon, Y. Dale, and Y. Yamamoto, *Phys. Rev. Lett.* **86**, 1502 (2001).
- ⁶P. Borri, W. Langbein, S. Schneider, U. Woggon, R. L. Sellin, D. Ouyang, and D. Bimberg, *Phys. Rev. Lett.* **87**, 157401 (2001).
- ⁷K. Matsuda, K. Ikeda, T. Saiki, H. Tsuchiya, H. Saito, and K. Nishi, *Phys. Rev. B* **63**, 121304(R) (2001).
- ⁸C. Kammerer, G. Cassabois, C. Voisin, C. Delalande, P. Roussignol, A. Lemaitre, and J. M. Gérard, *Phys. Rev. B* **65**, 033313(R) (2001).
- ⁹M. Bayer and A. Forchel, *Phys. Rev. B* **65**, 041308(R) (2002).
- ¹⁰I. Favero, G. Cassabois, R. Ferreira, D. Darson, C. Voisin, J. Tignon, C. Delalande, G. Bastard, P. Roussignol, and J. M. Gérard, *Phys. Rev. B* **68**, 233301(R) (2003).
- ¹¹L. Besombes, K. Kheng, L. Marsal, and H. Mariette, *Phys. Rev. B* **63**, 155307 (2001).
- ¹²P. Palinginis, H. Wang, S. V. Goupalov, D. S. Citrin, M. Dobrowolska, and J. K. Furdyna, *Phys. Rev. B* **70**, 073302(R) (2004).
- ¹³U. Bockelmann and G. Bastard, *Phys. Rev. B* **42**, 8947 (1990).
- ¹⁴R. Heitz, I. Mukhametzhanov, O. Stier, A. Madhukar, and D. Bimberg, *Phys. Rev. Lett.* **83**, 4654 (1999).
- ¹⁵M. Bissiri, G. B. vonHogersthal, A. S. Bhatti, M. Capizzi, A. Fropa, P. Frigeri, and S. Franchi, *Phys. Rev. B* **62**, 4642 (2000).
- ¹⁶O. Verzele, G. Bastard, and R. Ferreira, *Phys. Rev. B* **66**, 081308(R) (2002).
- ¹⁷T. Takagahara, *Phys. Rev. B* **60**, 2638 (1999).
- ¹⁸A. V. Uskov, A. P. Jauho, B. Tromborg, J. Mork, and R. Lang, *Phys. Rev. Lett.* **85**, 1516 (2000).
- ¹⁹B. Krummheuer, V. M. Axt, and T. Kuhn, *Phys. Rev. B* **65**, 195313 (2002).
- ²⁰E. A. Muljarov and R. Zimmermann, *Phys. Rev. Lett.* **93**, 237401 (2004).
- ²¹S. V. Goupalov, R. A. Suris, P. Lavallard, and D. S. Citrin, *IEEE J. Sel. Top. Quantum Electron.* **8**, 1009 (2002).
- ²²A. Vagov, V. M. Axt, and T. Kuhn, *Phys. Rev. B* **67**, 115338 (2003).
- ²³C. B. Duke and G. D. Mahan, *Phys. Rev.* **139**, 1965 (1965).
- ²⁴C. Kammerer, C. Voisin, G. Cassabois, C. Delalande, P. Roussignol, F. Klopff, J. P. Reithmaier, A. Forchel, and J. M. Gérard, *Phys. Rev. B* **66**, 041306(R) (2002).
- ²⁵P. Borri, W. Langbein, U. Woggon, V. Stavarache, D. Reuter, and A. D. Wieck, *Phys. Rev. B* **71**, 115328 (2005).
- ²⁶R. Oulton, A. I. Tartakovskii, A. Ebbens, J. Cahill, J. J. Finley, D. J. Mowbray, M. S. Skolnick, and M. Hopkinson, *Phys. Rev. B* **69**, 155323 (2004).
- ²⁷D. Lueerssen, R. Bleher, and H. Kalt, *Phys. Rev. B* **61**, 15812 (2000).
- ²⁸A. Olkhovets, R. C. Hsu, A. Lipovskii, and F. W. Wise, *Phys. Rev. Lett.* **81**, 3539 (1998).
- ²⁹S. Gopalan, P. Lautenschlager, and M. Cardona, *Phys. Rev. B* **35**, 5577 (1987).
- ³⁰S. Fafard, S. Rymond, G. Wand, R. Leon, D. Leonard, S. Charbonneau, J. L. Merz, P. M. Petroff, and J. E. Bowers, *Surf. Sci.* **361/362**, 778 (1996).

- ³¹R. Heitz, I. Mukhametzhano, A. Madhukar, A. Hoffmann, and D. Bimberg, *J. Electron. Mater.* **28**, 520 (1999).
- ³²G. Ortner, M. Schwab, M. Bayer, R. Passler, S. Fafard, Z. Wasilewski, P. Hawrylak, and A. Forchel, *Phys. Rev. B* **72**, 085328 (2005).
- ³³N. Koguchi, S. Takahashi, and T. Chikyow, *J. Cryst. Growth* **111**, 688 (1991).
- ³⁴K. Watanabe, N. Koguchi, and Y. Gotoh, *Jpn. J. Appl. Phys., Part 2* **39**, L79 (2000).
- ³⁵V. Mantovani, S. Sanguinetti, M. Guzzi, E. Grilli, M. Gurioli, K. Watanabe, and N. Koguchi, *J. Appl. Phys.* **96**, 4416 (2004).
- ³⁶M. Galluppi, A. Frova, M. Capizzi, F. Boscherini, P. Frigeri, S. Franchi, and A. Passaseo, *Appl. Phys. Lett.* **78**, 3121 (2001).
- ³⁷*Physics of Group IV Elements and III-V Compounds*, O. Madelung, Landolt-Börnstein New Series, Group III, Vol. 17, Pt. A (Springer, Berlin, 1982).
- ³⁸A. Ohtake, J. Nakamura, S. Tsukamoto, N. Koguchi, and A. Natori, *Phys. Rev. Lett.* **89**, 206102 (2002).
- ³⁹Y. Horikoshi, M. Kawashima, and H. Yamaguchi, *Jpn. J. Appl. Phys., Part 1* **27**, 169 (1988).
- ⁴⁰G. Ortner, D. R. Yakovlev, M. Bayer, S. Rudin, T. L. Reinecke, S. Fafard, Z. Wasilewski, and A. Forchel, *Phys. Rev. B* **70**, 201301(R) (2004).
- ⁴¹H. D. Robinson and B. B. Goldberg, *Phys. Rev. B* **61**, R5086 (2000).
- ⁴²V. Türck, S. Rodt, O. Stier, R. Heitz, R. Engelhardt, U. W. Pohl, D. Bimberg, and R. Steingrüber, *Phys. Rev. B* **61**, 9944 (2000).
- ⁴³K. Kuroda, T. Kuroda, K. Sakoda, G. Kido, and N. Koguchi (unpublished).
- ⁴⁴S. Rudin, T. L. Reinecke, and B. Segall, *Phys. Rev. B* **42**, 11218 (1990).
- ⁴⁵P. Borri, W. Langbein, J. M. Hvam, and F. Martelli, *Phys. Rev. B* **60**, 4505 (1999).
- ⁴⁶B. Urbaszek, E. J. McGhee, M. Kruger, R. J. Warburton, K. Karrai, T. Amand, B. D. Gerardot, P. M. Petroff, and J. M. Garcia, *Phys. Rev. B* **69**, 035304 (2004).
- ⁴⁷P. B. Allen and M. Cardona, *Phys. Rev. B* **23**, 1495 (1981).
- ⁴⁸E. Grilli, M. Guzzi, R. Zamboni, and L. Pavesi, *Phys. Rev. B* **45**, 1638 (1992).